HYDROTHERMAL SYNTHESIS OF FLOWER-LIKE $CoWO_4$ WITH GOOD SUPERCAPACITIVE PERFORMANCES

Xiao FAN, Xuyuan CHEN

Department of Microsystems, University of South-Eastern Norway, Campus Vestfold, Borre, Norway,
Xuyuan.Chen@usn.no

https://doi.org/10.37904/nanocon.2019.8691

Abstract

$CoWO_4$ is predicted to be a very promising electrode material for supercapacitors. In this study, a novel flower-like morphology of $CoWO_4$ fabricated by a hydrothermal method is presented for the first time. The prepared $CoWO_4$ have been thoroughly characterized by scanning electron microscopy and X-ray diffraction. The special $CoWO_4$ nanostructure exhibits noticeable specific capacitance of 156 $F \cdot g^{-1}$ at 0.5 $A \cdot g^{-1}$ and shows outstanding rate capability (85.2% capacitance retention at 10 $A \cdot g^{-1}$). The proposed feasible route is expected to be applied prospectively and widely in preparing $CoWO_4$ pseudocapacitive material, which owns great application value in supercapacitors.

Keywords: Supercapacitors, flower-like, $CoWO_4$, hydrothermal

1. INTRODUCTION

Nowadays, energy problems have become the greatest focus attracting the world's attention and triggering tremendous efforts for energy storage and conversion [1]. Numerous attentions have been paid to supercapacitors (SCs), also known as electrochemical capacitors (ECs), in recent years owing to their outstanding and unique abilities such as fast charge/discharge rate, high energy density, superior power density, long service life and environmental benignity [2-4]. Generally, SCs can be divided into two types, electrical double-layer capacitors (EDLCs) and pseudocapacitors (PCs), including two major categories of materials: carbonaceous materials and transition metal oxides/hydroxides, depending on their different charge storage mechanisms [5]. Due to higher levels of charge storage from redox reactions, PCs generate high specific capacitance that is often several times higher than that of EDLCs storing energy via reversible ion-absorption at the interface [6-7].

Previous literatures have reported that $CoWO_4$, one of the wolfram based salts, has excellent electrochemical activity. In addition, it also offers many advantages such as low cost, abundant resources and environmental friendliness [8-10]. Thus, $CoWO_4$ is predicted to be a very promising electrode material for SCs. However, there are scarce reports about $CoWO_4$ as electrode material candidate for SCs. The design and synthesis of novel morphologies to fully take advantage of $CoWO_4$ is still a key area of research. Moreover, the relationship between the structure and property is also worth investigating deeply. In this work, we reported a facile hydrothermal method, by which a flower-like $CoWO_4$ was obtained. The physical and chemical characterizations of the nanomaterial were systemically analyzed. The flower-like $CoWO_4$ displayed a high specific capacitance (154 $F \cdot g^{-1}$ at 5 $mV \cdot s^{-1}$, 156 $F \cdot g^{-1}$ at 0.5 $A \cdot g^{-1}$) with an outstanding rate capability (83.7% retention at 100 $mV \cdot s^{-1}$, 85.2% retention at 10 $A \cdot g^{-1}$). The unique nanostructured electrode material synthesized by this approach is economical and efficient, which manifests great potential for mass production and prospect for applications in energy storage further.

2. EXPERIMENTAL DETAILS

The chemicals were purchased from Sigma (U.S.A) and were of analytical grade and used without further purification. 1 mmol of $Co(NO_3)_2 \cdot 6H_2O$ and 1 mmol of $Na_2WO_4 \cdot 2H_2O$ were dissolved in 60 mL of deionized

water and stirred for 30 min. Subsequently, the resulting mixture was transferred to a Teflon-lined stainless-steel autoclave and heated at 150 ℃ for 10 h. The autoclave was cooled down to room temperature naturally. Finally, the sample was washed with deionized water and absolute ethanol successively and dried at 80 ℃ for 6 h. As-synthesized material was characterized using scanning electron microscope (SEM, Hitachi SU8230) and X-ray diffractometer (XRD, EQUINOX 1000).

The three-electrode system was employed to evaluate electrochemical properties of the obtained $CoWO_4$. The working electrode was fabricated by pressing a slurry onto nickel foam (NF). The slurry was prepared by dispersed the 80 wt% of $CoWO_4$, 15 wt% of acetylene black, and 5 wt% of polyvinylidene fluoride (PVDF) in n-methyl-2-pyrrolidone (NMP) solvent. The working electrode was dried at 80 ℃ overnight before test. The measurements consisting of cyclic voltammogram (CV) at various scan rates, galvanostatic charge/discharge (GCD) at different current densities and electrochemical impedance spectrum (EIS) in frequency range from 100 mHz to 100 kHz were performed on a Zahner IM6 electrochemical workstation, where 2 M KOH, Pt net and Ag/AgCl served as electrolyte, counter electrode and reference electrode, respectively.

The specific capacitance based on CV [11] is defined as

$$C = \frac{\int i(V)\mathrm{d}V}{2mv\Delta V} \quad (1)$$

The specific capacitance based on GCD [11] is given by

$$C = \frac{It}{m\Delta V} \quad (2)$$

where:

C - the specific capacitance (F·g)

$\int i(V)\mathrm{d}V$ - the integrated area of CV curve (V·A)

m - the mass of active material (g)

v - the scan rate ($V \cdot s^{-1}$)

ΔV - the potential window (V)

I - the discharge current (A)

t - the discharge time (s)

3. RESULTS AND DISCUSSION

The surface morphologies and microstructure characters of as-synthesized $CoWO_4$ were imaged by SEM with different magnifications. Abundant nanosheet-assembled flower-like nanostructures presented by **Figure 1a** with good monodispersity and uniformity are observed clearly. No other morphologies can be detected, demonstrating a high yield. The enlarged SEM image shown in **Figure 1b**

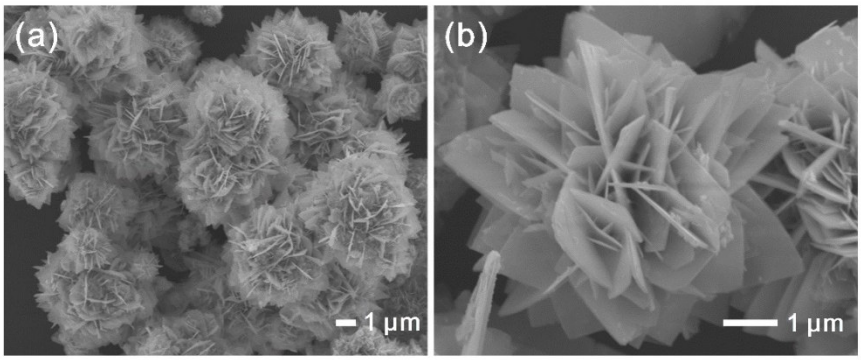

Figure 1 SEM images of (**a**) low- and (**b**) high-magnification of the $CoWO_4$

reveals that the 3D hierarchical architecture is constructed with dozens of 2D nanosheets with smooth surfaces, which significantly increases the specific surface area. Obviously, the increased number of exposed active sites can enhance the utilization efficiency of the active material. Furthermore, the unique structure as ion-buffering reservoir [12] can provide a short diffusion distance and facilitate the rapid transport of electrolyte ions to the interior of bulk material. Based on the above results, the flower-like structure possibly leads to superior electrochemical performances.

To further investigate the formation of the sample, the XRD patterns were given in **Figure 2**. The sharp diffraction peak at 30.6° corresponds to the reflection of (-111) plane. The other diffraction peaks at 15.6°, 19°, 23.8°, 24.7°, 36.2°, 38.5°, 41.2°, 54° and 65° can be assigned to the reflections of (010), (001), (-110), (011), (200/120), (002), (-201), (-202), and (-231) planes, respectively. The observed diffraction peaks are well indexed and matched to the monoclinic structure phase of $CoWO_4$ with standard patterns (JCPDS card No.15-0867). The sharp and narrow diffraction peaks reveal that the obtained $CoWO_4$ has high crystal degree [13,14]. Moreover, there are no peaks leaded by impurities or other residuals, which indicates the high purity of the product.

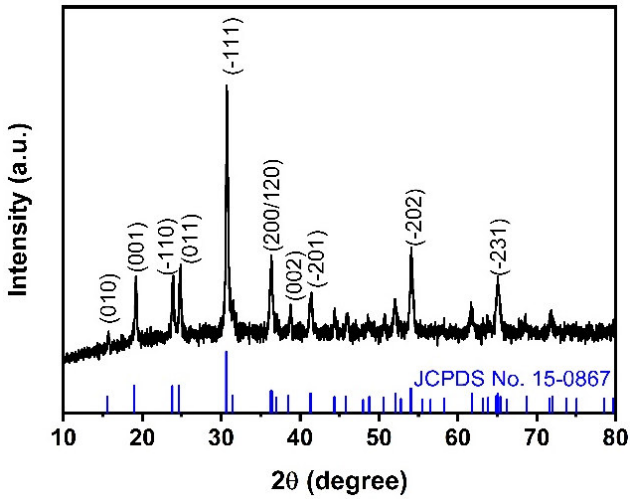

Figure 2 XRD patterns of the $CoWO_4$

Electrochemical properties of the flower-like $CoWO_4$ as electrode material for SCs were evaluated systematically. **Figure 3a** shows CV curves of the $CoWO_4$ at various scan rates within a potential window of 0-0.5 V. As expected, differing from the ideal rectangular shape for EDLCs, typical pseudocapacitive CV curves with distinct and nearly symmetrical pair of redox peaks are presented, indicating that the measured capacitance is mainly governed by faradaic redox mechanism. The reaction is based on reversible redox of Co^{2+} to Co^{3+} associated with OH^- anions. Additionally, the main function of W in $CoWO_4$ is to improve the conductivity of the material rather than involve in redox reaction and contribute to the capacitance [15]. When the scan rate increases from 5 to 100 $mV{\cdot}s^{-1}$, the peak currents increase enormously and the anodic peaks shift towards positive potential, while the cathodic peaks move towards negative potential. Notably, the shapes of CV curves do not deliver significant distortion. In other words, the $CoWO_4$ at 100 $mV{\cdot}s^{-1}$ still can keep a similar redox shape compared to the original shape at 5 $mV{\cdot}s^{-1}$, revealing rapid current-voltage response and ideal electrochemical behavior.

The specific capacitance is the most important parameter to evaluate the electrochemical performance of SCs. According to equation (1), the high specific capacitance of 154 $F{\cdot}g^{-1}$ can be estimated at the scan rate of 5 $mV{\cdot}s^{-1}$. Owing to the movement of the electrolyte ions (OH^-) limited by time constraint at high scan rate charge/discharge process [16], the specific capacitances of the $CoWO_4$ gradually decrease as the scan rate

increases. It is noteworthy to mention that the inevitably decrease of specific capacitances exhibits a gentle curve, as illustrated in **Figure 3b**. The capacitance retention rate is 83.7% at 100 mV·s^{-1} compared with the specific capacitance at 5 mV·s^{-1}.

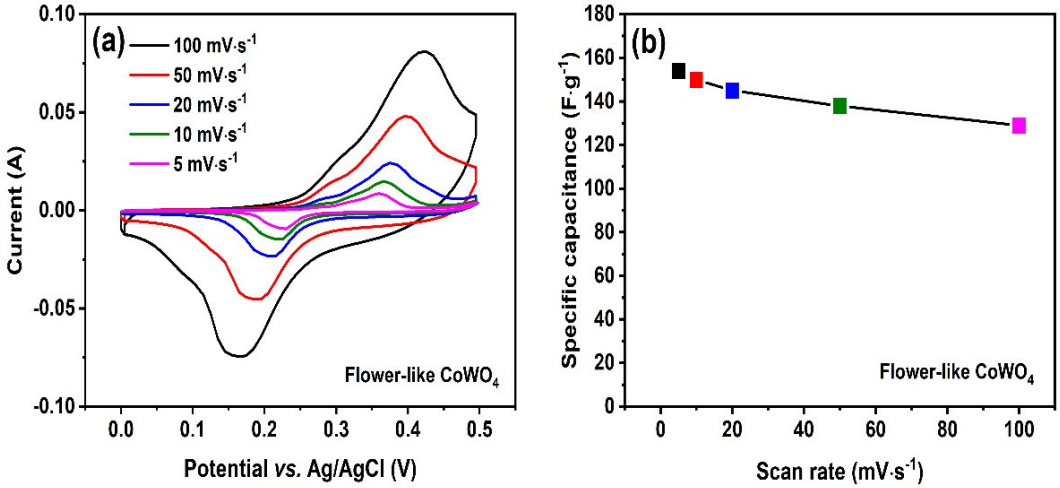

Figure 3 (**a**) CV curves and (**b**) specific capacitances of the $CoWO_4$ electrode

GCD tests at different current densities in a voltage range of 0-0.5 V were performed. In comparison with the discharge curves of EDLCs (close to straight line), evident plateaus corresponding to the redox reaction described by Co^{2+} to Co^{3+} are observed, as displayed in **Figure 4a**. On the basis of equation (2), the specific capacitance is calculated to be 156 F·g^{-1} at the current density of 0.5 A·g^{-1}. Due to the correlation between diffusion rate of electrolytic ions into the electrode material and current density, the boost of current densities would result in fading in the capacitance values (**Figure 4b**) [1,17]. The capacitance retention rate is 85.2% at 10 A·g^{-1} compared with the specific capacitance at 0.5 A·g^{-1}.

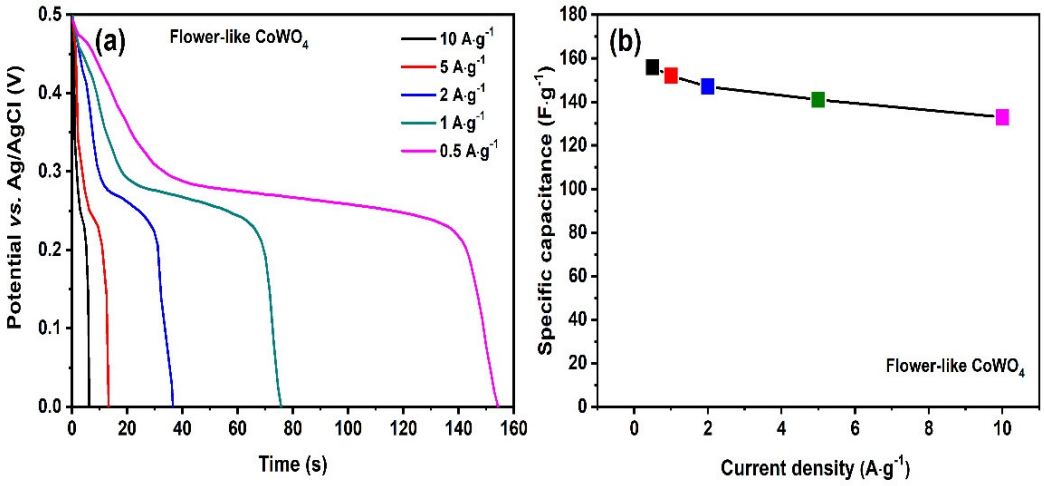

Figure 4 (**a**) Discharge curves and (**b**) specific capacitances of the $CoWO_4$ electrode

EIS is a very powerful measurement for providing information about the frequency response of the $CoWO_4$ modified electrode. As depicted in **Figure 5**, in the high frequency region, the first intersection point with the real axis of Nyquist plot reflects the equivalent series resistance (ESR, 0.5 Ohm) including the resistance of electrolyte solution, the intrinsic resistance of active material, and the contact resistance of interface active

material/current collector. The small ESR is due to the unique structure facilitating the efficient access of electrolyte ion to active material surface and shortening the ion diffusion path [18,19]. Meanwhile, no distinct semicircle can be observed, expressing fast ions diffusion towards the $CoWO_4$ modified electrode. In the low frequency range, the plot presents a straight line with a slope of 45°, which implies relatively typical capacitor behavior [19].

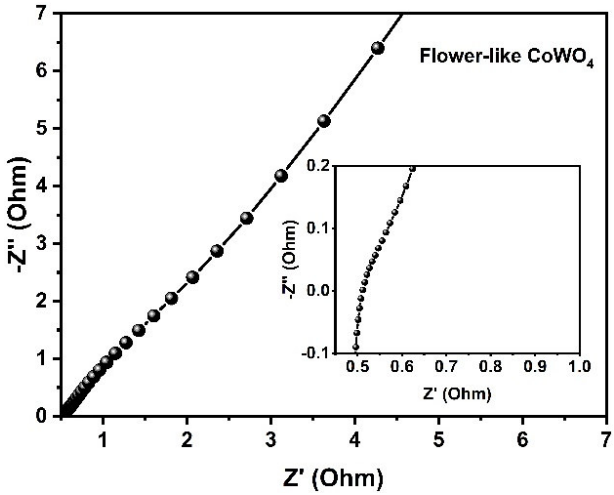

Figure 5 EIS plot of the $CoWO_4$ electrode

4. CONCLUSION

In summary, flower-like $CoWO_4$ was successfully prepared by a simple approach and characterized in detail. The $CoWO_4$ in this work possesses good supercapacitive performances (156 $F \cdot g^{-1}$ at 0.5 $A \cdot g^{-1}$ accompanying limited decay of 14.8% at 10 $A \cdot g^{-1}$). The high specific capacitance and remarkable rate capability leaded by its unique flower-like structure make it promising for application in supercapacitors. The current work also may encourages a broad application range of $CoWO_4$ such as electrochemical sensing and lithium ion batteries.

REFERENCES

[1] WANG, Y., LEI, Y., LI, J., GU, L., YUAN, H. and XIAO, D. Synthesis of 3D-nanonet hollow structured Co_3O_4 for high capacity supercapacitor. *ACS applied materials & interfaces*. 2014. vol. 6, iss. 9, pp. 6739-6747.

[2] HE, G., LI, J., LI, W., LI, B., NOOR, N., XU, K., HU, J. and PARKIN, I. P. One pot synthesis of nickel foam supported self-assembly of $NiWO_4$ and $CoWO_4$ nanostructures that act as high performance electrochemical capacitor electrodes. *Journal of Materials Chemistry A*. 2015. vol. 3, iss. 27, pp. 14272-14278.

[3] SIMON, P., GOGOTSI, Y. and DUNN, B. Where do batteries end and supercapacitors begin?. *Science*. 2014. vol. 343, iss. 6176, pp. 1210-1211.

[4] KÖTZ, R. and CARLEN, M.J.E.A. Principles and applications of electrochemical capacitors. *Electrochimica acta*. 2000. vol. 45, iss. 15-16, pp. 2483-2498.

[5] WANG, C., ZHOU, E., HE, W., DENG, X., HUANG, J., DING, M., WEI, X., LIU, X. and XU, X. $NiCo_2O_4$-based supercapacitor nanomaterials. *Nanomaterials*. 2017. vol. 7, iss. 2, pp. 41.

[6] LU, P., OHLCKERS, P., MÜLLER, L., LEOPOLD, S., HOFFMANN, M., GRIGORAS, K., AHOPELTO, J., PRUNNILA, M. and CHEN, X. Nano fabricated silicon nanorod array with titanium nitride coating for on-chip supercapacitors. *Electrochemistry Communications*. 2016. vol. 70, pp. 51-55.

[7] LIU, J., JIANG, J., CHENG, C., LI, H., ZHANG, J., GONG, H. and FAN, H.J. Co_3O_4 nanowire@MnO_2 ultrathin nanosheet core/shell arrays: a new class of high-performance pseudocapacitive materials. *Advanced Materials*. 2011. vol. 23, iss. 18, pp. 2076-2081.

[8] WANG, Y., SHEN, C., NIU, L., SUN, Z., RUAN, F., XU, M., SHAN, S., LI, C., LIU, X. and GONG, Y. High rate capability of mesoporous $NiWO_4$-$CoWO_4$ nanocomposite as a positive material for hybrid supercapacitor. *Materials Chemistry and Physics*. 2016. vol.182, pp. 394-401.

[9] XU, X., SHEN, J., LI, N. and YE, M. Facile synthesis of reduced graphene oxide/$CoWO_4$ nanocomposites with enhanced electrochemical performances for supercapacitors. *Electrochimica Acta*. 2014. vol. 150, pp. 23-34.

[10] KUMAR, R.D. and KARUPPUCHAMY, S. Microwave mediated synthesis of nanostructured Co-WO_3 and $CoWO_4$ for supercapacitor applications. *Journal of Alloys and Compounds*. 2016. vol. 674, pp. 384-391.

[11] LU, P., HALVORSEN, E., OHLCKERS, P., MÜLLER, L., LEOPOLD, S., HOFFMANN, M., GRIGORAS, K., AHOPELTO, J., PRUNNILA, M. and CHEN, X. Ternary composite Si/TiN/MnO_2 taper nanorod array for on-chip supercapacitor. *Electrochimica Acta*. 2017. vol. 248, pp. 397-408.

[12] WANG, Q., YAN, J., WANG, Y., WEI, T., ZHANG, M., JING, X. and FAN, Z. Three-dimensional flower-like and hierarchical porous carbon materials as high-rate performance electrodes for supercapacitors. *Carbon*. 2014. vol. 67, pp. 119-127.

[13] XING, X., GUI, Y., ZHANG, G. and SONG, C. $CoWO_4$ nanoparticles prepared by two methods displaying different structures and supercapacitive performances. *Electrochimica Acta*. 2015. vol. 157, pp. 15-22.

[14] ZHANG, M., FAN, H., ZHAO, N., PENG, H., REN, X., WANG, W., LI, H., CHEN, G., ZHU, Y., JIANG, X. and WU, P. 3D hierarchical $CoWO_4$/Co_3O_4 nanowire arrays for asymmetric supercapacitors with high energy density. *Chemical Engineering Journal*. 2018. vol. 347, pp. 291-300.

[15] XU, X., GAO, J., HUANG, G., QIU, H., WANG, Z., WU, J., PAN, Z. and XING, F. Fabrication of $CoWO_4$@$NiWO_4$ nanocomposites with good supercapacitve performances. *Electrochimica Acta*. 2015. vol. 174, pp. 837-845.

[16] GUO, D., SONG, X., LI, F., TAN, L., MA, H., ZHANG, L. and ZHAO, Y. Oriented synthesis of Co_3O_4 core-shell microspheres for high-performance asymmetric supercapacitor. *Colloids and Surfaces A: Physicochemical and Engineering Aspects*. 2018. vol. 546, pp. 1-8.

[17] WANG, X., ZHANG, N., CHEN, X., LIU, J., LU, F., CHEN, L. and SHAO, G. Facile precursor conversion synthesis of hollow coral-shaped Co_3O_4 nanostructures for high-performance supercapacitors. *Colloids and Surfaces A: Physicochemical and Engineering Aspects*. 2019. vol. 570, pp. 63-72.

[18] LU, P., MÜLLER, L., HOFFMANN, M. and CHEN, X. Taper silicon nano-scaffold regulated compact integration of 1D nanocarbons for improved on-chip supercapacitor. *Nano Energy*. 2017. vol. 41, pp. 618-625.

[19] WANG, Q., WANG, X., LIU, B., YU, G., HOU, X., CHEN, D. and SHEN, G. $NiCo_2O_4$ nanowire arrays supported on Ni foam for high-performance flexible all-solid-state supercapacitors. *Journal of Materials Chemistry A*. 2013. vol. 1, iss. 7, pp. 2468-2473.